SI ENCOM2017

Corresponding author info:

Jan N. Geiler, Gasoline Systems, Robert-Bosch-Campus 1, D-71272 Renningen, Baden-Württemberg, Germany, Email: Jan.Geiler@de.bosch.com.

Development of laser-induced fluorescence (LIF) to quantify in-cylinder fuel wall-films

Jan N. Geiler[1], Roman Grzeszik[1], Sebastian Quaing[1], Andreas Manz[1], Sebastian A. Kaiser[2]

[1] Laboratory Mixture Formation and Combustion, Gasoline Systems, Robert Bosch GmbH, Robert-Bosch-Campus 1, 71272 Renningen, Germany.

[2] Institute for Combustion and Gas Dynamics – Reactive Fluids, University of Duisburg-Essen, Lotharstr. 1, 47057 Duisburg, Germany.

Abstract

Laser-induced fluorescence (LIF) of a fuel tracer is a very sensitive technique to image in-cylinder liquid fuel films, but quantification of the measured film thickness has proven difficult so far. This paper describes improvements in the quantification procedure and presents an example application in a motored, optically accessible spark-ignition engine with direct injection. We designed a calibration tool that could be pressurized and heated, allowing investigation of the LIF intensities at temperatures exceeding the liquid's standard-pressure boiling point. The fluorescence intensity of liquid toluene and 3-pentanone dissolved in iso-octane upon excitation with a pulsed laser at 266 nm was investigated as a function of temperature and pressure. Consistent with literature results on gas-phase LIF, the signal from toluene was much stronger than from 3-pentanone, about two orders of magnitude for films thinner than 50 µm. LIF from both tracers decreased with increasing temperature, but that of toluene significantly more. The response to pressure was less pronounced. For imaging across a large field of view, the spatial non-uniformity of laser excitation and detection efficiency was taken into account using a solid fluorescing substrate, an inexpensive Schott-glass WG280 filter. Iso-octane with 0.5 vol.-% toluene was used for application in the motored engine, imaging the liquid film on the piston-top window after direct injection from a central multi-hole injector. Air as a bulk gas was found to be advantageous over nitrogen in that gas-phase fluorescence was quenched by oxygen. The imaged film distributions and

thicknesses and the derived total fuel-film mass were physically plausible. Consistent with recent literature results from a constant-pressure vessel, increasing injection pressure from 50 to 100 bar did not decrease wall wetting, but further increase to 200 bar did.

Keywords

LIF, laser-induced fluorescence, optical diagnostics, fuel wall-film, toluene, 3-pentanone, tracer, film thickness

Introduction

With introduction of the Euro 6c emission standard in 2017, the limit for the number of emitted particles (PN) from gasoline engines with direct injection is lowered to 6×10^{11} particles per kilometer. With gasoline direct-injection (GDI) engines, it is challenging to comply with this limit, especially in tests representing "real" driving conditions. Therefore, an improved understanding of particle formation inside of the combustion chamber of gasoline engines is urgently needed. Ideally, this would occur through a non-intrusive technique with high spatial and temporal resolution. Endoscopic in-cylinder imaging has qualitatively shown that particle formation is correlated with locally rich mixture zones [1]. These zones arise from fuel-concentration inhomogeneities in the gas phase or from fuel wall films, e.g. thin layers of liquid fuel on the cylinder liner or piston surface due to wall impingement of the fuel spray. Drake et al. [2] found pool fires on the piston to be the dominant source of smoke emissions from their engine. From optical film-thickness measurements (discussed below), they estimated that 10 % of the fuel-film's mass was converted to engine-out smoke. High-speed two-color pyrometry coupled with OH*-luminescence imaging clearly showed the persistence of pool-fire soot long after the disappearance of soot radiation from the main gas-phase combustion [3]. To identify the location and – a much more challenging task – to quantify the thickness of thin fuel films, a sensitive optical measurement technique is required. One option is laser-induced fluorescence (LIF), which is an established diagnostic for determining the local air/fuel ratio in the gas phase [4, 5, 6, 7, 8]. This very sensitive method has the potential to detect even small amounts of liquid fuel inside the intake manifold of engines with port fuel injection (PFI) [9, 10] or the combustion chamber of engines with gasoline direct injection (GDI) [11, 12, 13]. However, quantification of the LIF signal at elevated pressures and temperatures still needs improvement. This is because various interacting parameters influence the detected signal.

Optical detection of fuel films in engines

In principle, several measurement techniques based on gravimetric, capacitive, conductive, acoustic, or optical detection are able to determine the thickness of a liquid film on a solid substrate. An overview of techniques for film-thickness measurements is given by the reviews of Tibiriça et al. [14] and Al-Sibai [15]. Gravimetric measurements are not practical in an engine and do not deliver spatially resolved data. Ultrasonic imaging appears to be unsuitable for application in an engine, because the measurement uncertainty is too high for thin films. The low conductivity and the low dielectric

constant of fuels make it difficult to apply measurements based on capacity or conductivity [16, 17].

Optically accessible research engines are often used to investigate the physical-chemical processes in IC engines in detail. Indeed, several optical diagnostics have been used for fuel-film visualization.

In the infrared (IR) region of the spectrum, Schulz et al. [18] performed black-body emission imaging of the temperature reduction caused by the impingement of the spray on an electrically heated wall. However, the metallic (or fused silica) surfaces in the cylinder cannot be treated as a black body. Hydrocarbon fuels absorb IR light over broad wavelength regions. By measuring the attenuation of transmitted IR light, it would be possible to detect even thin wall films. A disadvantage is that optical access to the combustion chamber from two opposing sides is needed for a transmission measurement. Absorption by the gas phase next to the film may also be an issue [14,19].

Refractive index matching (RIM) is a more practical option for fuel-film imaging. In engines, it has been applied by Drake et al. [2], Fansler and Drake [20], and Schropp and Grzeszik [11, 12]. RIM exploits the fact that on a rough transparent surface (e.g., the optical engine's piston-top window), light is reflected more diffusely when that surface is dry than when it is wet. Thus, the measurement range is restricted to film thicknesses less than the roughness of the window surface. In previous measurements [2, 20], practically detectable film thicknesses were in the range from 30 nm to 3.5 µm. Fuel wall films may be much thicker than that but to a certain extent the window roughness could be adjusted.

In in-cylinder measurements, laser-induced fluorescence (LIF) is an established technique for detecting fuel in the gas-phase [8], but application of LIF to liquid films has been far less frequent. Maligne and Bruneaux [21] compared fuel-film thicknesses obtained by RIM and by LIF. They found strong qualitative similarity between the results.

As early as 1964, liquid film measurements based on fluorescence were conducted by Hewitt [22]. Later, Le Coz and Baritaud [19] investigated fuel films in the intake manifold of PFI engines point-wise, followed by others e.g. [23], 24]. By means of LIF, the measurable film thicknesses range from 5 µm to 1.5 mm [14, 11]. The measurements of Senda [23] delivered spatially resolved fuel-film thicknesses in the intake manifold. Because high temperatures and pressures may influence the fluorescence signal, quantitative LIF imaging inside the combustion chamber of GDI engines is much more challenging. From gas-phase LIF it is known that for quantification detailed understanding of the underlying photophysics is necessary [8]. Efforts towards quantitative LIF measurements of fuel films in optically accessible engines were made by e.g. Lin and Sick [13], Stevens et al. [25], Schropp [11], Kull et al. [26], and Cho and Min [34]. By transmitting and collecting the light from below the piston, the liquid on the pistons surface could be imaged. However, Lin and Sick [13] found distinction between fluorescence from the liquid and the gas phase to be problematic in quantitative evaluation of the fuel-film thicknesses.

Kay et al. [27] and recently Schulz et al. [28, 29] describe work to determine the wall film thickness in a constant volume chamber. 3-pentanone was chosen as a fluorescent tracer, because its fluorescence quantum yield was assumed to be independent of temperature, pressure, and oxygen concentration [30]. However, the fluorescence signal from 3-pentanone is low compared to that from toluene [13, 31]. In addition, preferential

evaporation of 3-pentanone was found, resulting in an underestimation of the film thickness [32].
Lin and Sick [13], and Kay et al. [27] identified the fluorescence coming from the already evaporated fuel in the gas phase as a possible source of error. This could be eliminated by TIR-LIF (total internal reflection LIF), as conducted by Alonso et al. [33] on a fused silica plate as a substrate. However, for this method, the laser beam needs to be directed into the substrate laterally. This is possible for measurements on the cylinder liner [34], but would be challenging for the piston top.
Lin and Sick [13], as well as Schropp and Grzeszik [11, 12] conducted quantitative investigations of the wall film thickness on the piston surface in an optical engine with direct injection. They motored the engine and used nitrogen instead of air as the charge gas, minimizing possible quenching by oxygen. The influence of such quenching on the gas phase next to the film and on the film itself (via diffusion of into the spray's droplets) was not investigated. By comparing data obtained with aromatics and 3-pentanone as a tracer in isooctane, Stevens and Steeper [25] and [13] found a significant effect of quenching on the liquid phase.
Recently, Schulz et al. [28] gave an excellent overview of the accuracy attainable with LIF. Besides various error sources, different calibration methods were discussed in terms of their accuracy. In order to minimize the calibration error, they suggested a thickness calibration at realistic values. Calibration at elevated temperatures and pressures was not conducted, instead it was assumed that the fluorescence signal from 3-pentanone is not affected by either. In a subsequent study, the same group [29] investigated fuel-film thicknesses at different injection pressures, injection timings, and gas pressures in a vessel, simulating engine conditions.
In order to investigate the effects of wall films on the formation of particles, it is necessary to develop LIF for conditions as close as possible to real operating conditions. In this work, the calibration is separated in two steps, a relative flat-field correction and an absolute film-thickness calibration. The flat-field correction accounts for the spatially varying sensitivity of the laser-camera system over the entire field of view (FOV) and is based on fluorescence from a solid disk, not a liquid film. The absolute calibration determines the fluorescence signal over a relatively small area, for which a known liquid film thickness can be accurately produced in a calibration device. We designed a device that can be pressurized and heated, allowing for investigation of the influence of pressure and temperature on fluorescence. In particular it is possible to quantify the relative LIF signal at temperatures exceeding the liquid's standard-pressure boiling point, which is very relevant in the compressions stroke.

Basic principle of LIF for fuel-film detection

In LIF, laser light is absorbed by a molecule or atom, exciting it to a higher electronic state. To return to the ground state, the energy can be released through radiative processes (e.g. fluorescence, phosphorescence) or non-radiative processes (e.g. collisional energy transfer to other molecules, "quenching") [35]. Due to rotational-vibrational relaxation prior to fluorescence, the fluorescence photon is of lower energy than the absorbed (laser) photon, thus the fluorescence is red-shifted (Stokes shift, [35]) with respect to the

excitation wavelength. This facilitates separating the fluorescence signal from scattered excitation (laser) light by spectral filters.
Commercial fuels contain many compounds that strongly fluoresce when excited with UV light. However, it is difficult to quantitatively relate the measured fluorescence to the amount of fuel it originates from because so many species, most with unknown fluorescence properties, occur in commercial fuels. Thus, for quantifiable LIF measurements, a fluorescent tracer is added at low concentration to a non-fluorescing fuel surrogate.
For weak incident light intensity (and under other simplifying assumptions), the fluorescence intensity I_f is in proportional to the intensity of absorbed light I_a, as described by equation (1). The fluorescence quantum yield ϕ describes the ratio of emitted to absorbed photons and η is the efficiency of the detection system. I_a can be expressed as the difference between the laser-light intensity I_0 incident on the medium and the transmitted intensity I_t. In the medium, I_t follows an exponential decay, the Lambert–Beer law, with the absorber concentration c, the extinction coefficient ϵ^*, and the path length d in the exponent. In our case, c is the concentration of the tracer and d is the quantity of interest, the film thickness.

$$I_f = \eta\ \phi\ I_a = \eta\ \phi\ (I_0 - I_t) = \eta\ \ \phi\ I_0\ (1 - \exp(-\epsilon^* c\ d)) \quad (1)$$

If the product $\epsilon^* c\ d$ is small, equation (1) can be approximated in first order by a linear function, and the fluorescence detected from the fluorescent absorber is then linearly dependent on the film thickness:

$$I_f \approx \eta\ \phi\ I_0\ \epsilon^*\ c\ d \quad (2)$$

The fluorescence quantum yield ϕ and the extinction coefficient ϵ^* may be functions of temperature and pressure [8]. In particular, collisional quenching by oxygen molecules may reduce ϕ. From gas-phase tracer-LIF measurements it is known that the besides the concentration of the quencher, the effect of quenching also depends on the temperature [38]. For quantitative imaging of the fuel-film thickness, all factors preceding d in equation (2) need to be known or taken into account by additional calibration. Like the measurement itself, in imaging this calibration is performed pixel-wise across the FOV.

Bench-top testing

Experiment

Figure 1 shows the optical system for LIF-based film-thickness measurements. A frequency-quadrupled Nd:YAG-laser (component 1) at 266 nm (10 Hz, 60 mJ/pulse) serves as light source. Mirror (2) reflects only the desired wavelength, 266 nm, transmitting residual light at 532 nm and 1064 nm into a beam dump (3). The laser pulse energy can be adjusted by a polarization-based attenuator (4). An energy monitor (5) measures and logs the energy of a 5 %-reflection of each laser pulse to later correct for temporal fluctuations of the total laser energy. The beam is expanded by a plano-concave lens (6, focal length f=-50 mm). An aperture (7) restricts the irradiated area to avoid

undesired reflections and two mirrors (8+9) guide the widened laser beam through the piston's silica-glass window (10) into the probe volume (11).
The emitted fluorescent light is detected via reflection by mirror (9) and transmission through the dichroic mirror (8, spectral characteristics in Figure 10) by an intensified CCD-camera (13, LaVision NanoStar, S20 cathode) with lens (100 mm, set to f/5.6). Additional suppression of scattered laser light is achieved by a 266 nm long-pass filter (12). The projected pixel size of the camera system is 0.09 mm/pixel.

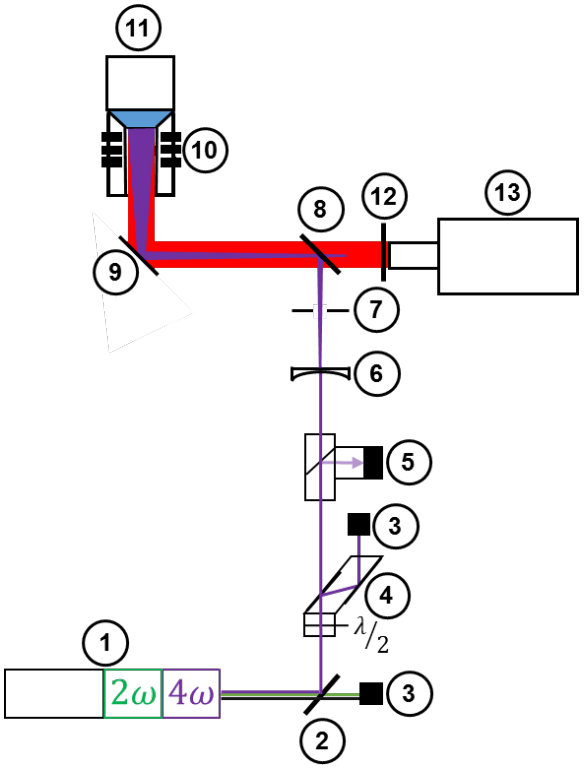

Figure 1. Optics and beam path in the experiments. The numbered elements are discussed in the text.

Calibration and flat-field correction

To quantify the fuel film thickness by LIF, the fluorescence signal has to be calibrated. With known fluorescence intensity $I_{\mathrm{f,ref}}$ of a reference fuel-film with thickness d_{ref}, the film thickness d_{exp} can be determined at the coordinates x and y via equation (3) from the experimentally detected fluorescence intensity $I_{\mathrm{f,exp}}$:

$$d_{\mathrm{exp}}(x,y) = d_{\mathrm{ref}}(x,y)\frac{I_{\mathrm{f,exp}}(x,y)}{I_{\mathrm{f,ref}}(x,y)}\frac{\eta_{\mathrm{ref}}(x,y)}{\eta_{\mathrm{exp}}(x,y)}\frac{\phi_{\mathrm{ref}}}{\phi_{\mathrm{exp}}}\frac{I_{0,\mathrm{ref}}(x,y)}{I_{0,\mathrm{exp}}(x,y)}\frac{\epsilon^*_{\mathrm{ref}}}{\epsilon^*_{\mathrm{exp}}}\frac{c_{\mathrm{ref}}(x,y)}{c_{\mathrm{exp}}(x,y)} \qquad (3)$$

For calibration with defined liquid film thicknesses d_{ref}, a suitable calibration device is needed.
Equation (3) indicates that the fluorescence intensity depends on the intensity of the exciting laser light. The temporal fluctuations of the total laser-pulse energy are taken into account by the energy monitor. However, the laser intensity is not uniform across the

camera's FOV on the probe. Calibration over the entire FOV (here, the piston top window with a diameter of 56 mm) is necessary, but producing a µm-thin liquid film that is uniform over a large area is difficult. Therefore, for quantification we separate absolute thickness calibration from "flat-fielding", i.e., correction of variations in local system response (laser intensity and detection efficiency).

Absolute calibration

For absolute calibration and for general investigations of liquid-phase tracer-LIF a calibration device was designed. Figure 2 shows the two versions of this device.
Version 1 (Figure 2(a)) is more compact to fit into the optical engine, and operates at room temperature and ambient pressure. It allows setting film thicknesses from 10 to 300 µm and hence finding the correlation between the detected LIF signal and the fuel-film thickness. This range covers the expected films on the piston surface under cold-start conditions [9, 10]. The liquid is supplied by connectors (1) and (2) to the probe volume between the two fused silica plates (4). The front and back windows are separated by thin precision shims (3) that determine the film thickness. The optically accessible diameter of the device is 30 mm.
Version 2 is shown in Figure 2(b). It is larger and thus more suitable for bench-top experiments, but it can operate at elevated temperature and pressure. Here, the back plate (5) is metal, transferring heat to the film from a temperature-control circuit (connectors 6 and 7) filled with silicone oil. A maximum temperature of 180 °C is possible. The liquid film is pressurized up to 16 bar by nitrogen through connectors (1) and (2). This combination of temperature and pressure allows covering almost the entire boiling curve of typical gasoline and corresponding tracer-doped surrogate fuels while keeping the fuel in the liquid phase.
Space allowing, in-situ calibration with Version 2 at a temperature and pressure close to the anticipated in-cylinder conditions is preferable. However, in our optical engine the space constraints are such that only Version 1 fits. Transfer of the calibration to elevated temperature and pressure then is achieved by additional bench-top measurements with Version 2.

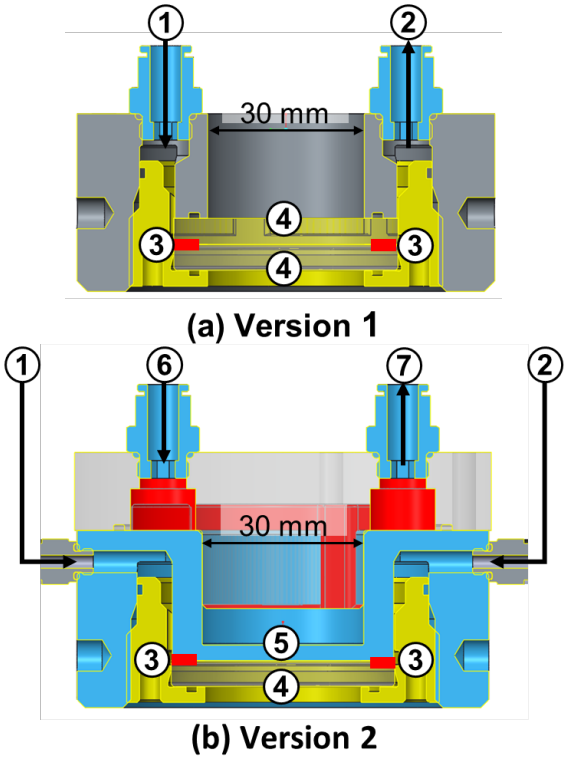

Figure 2. Two versions of the calibration tool. The numbered elements are discussed in the text. Typically, the direction of laser irradiation and fluorescence detection are from the bottom.

Flat-field correction

For the flat-field correction, a probe volume with spatially uniform response to LIF excitation is needed. Various materials were tested for their suitability, commercial overhead transparency film, glass (thickness: 10 mm), and four different Schott-glass long-pass filters, WG280, WG295, WG305, and WG320 (thickness: 2 mm).
To investigate the fluorescence spectra from the different potential flat-field materials, the camera (component 13 in Figure 1) was mounted at the exit plane of a grating spectrograph (Oriel MS260i, 50 lines/mm, blazed at 300 nm, resolution 2 nm). The measured peak-normalized fluorescence spectra are given in Figure 3. They differ significantly. Emission from the glass is spectrally broadest. The overhead transparency film and the WG320 have their maximum emission in the visible wavelength range, at about 410 and 450 nm, respectively, while the three other long-pass filters WG280, WG295, and WG305 have a distinctive peak at 350 nm. That of the WG280 filter is the narrowest, with the least of the spectrum extending into the visible.

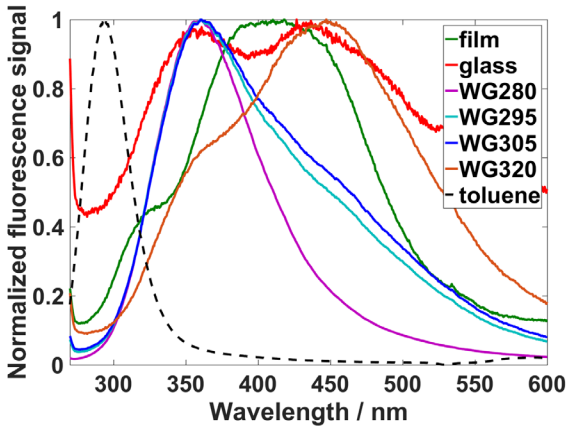

Figure 3. Fluorescence spectra from the flat-field material candidates upon excitation at 266 nm.

Quantification according to equations (1 – 3) is simplified if the quantum efficiency ϕ is independent from the incident laser intensity I_0. To test this for the potential flat-field materials, the incident laser fluence was varied between 0.03 and 0.6 mJ/cm² via the beam attenuator (component 4 in Figure 1). The corresponding measured fluorescence signal is plotted in Figure 4. Fluorescence from WG320 and glass is the weakest, WG295 and WG305 fluoresce stronger, and the highest signals are found for the transparency film and the WG280 filter. However, for the film the signal is not linearly dependent on the laser fluence over much of the examined range of fluences.

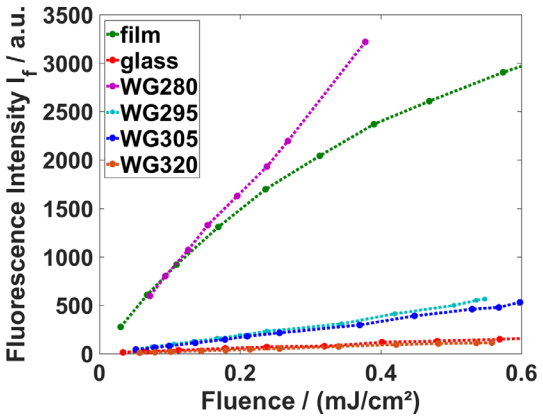

Figure 4. Fluorescence intensities from the flat-field material candidates as a function of laser fluence.

Additionally, the materials were tested for their long-term stability against UV-laser irradiation. With exception of the overhead transparency film, all materials showed constant fluorescence signal over approximately 180 minutes of irradiation at 10 Hz repetition rate and a fluence of 0.6 mJ/cm².

Because of its strong, stable fluorescence signal in a wavelength range nearby the maximum fluorescence intensity of toluene (and other aromatics), the WG280 filter was chosen for further use. Note that the filters are manufacturer-specified for their *transmission*, while *fluorescence* is not specified and may differ between manufacturers

and maybe even glass melts. Thus, their suitability for a “toluene-like” flat-field material needs to be experimentally examined before use.

Post-processing of images from the calibration devices

The LIF images of the WG280 filter were used to correct for the system response (laser, camera) when imaging the liquid thin film. Four ensembles of images are acquired for each measurement. Examples of a set of ensemble-averages are shown in Figure 5(a) to (d). These images are used as follows:

1. Normalize each image with respect to the laser energy of the corresponding pulse as measured by the energy monitor (component 5 in Figure 1).
2. Subtract an ensemble-averaged background image BG_1 (Figure 5(a)) from the corresponding averaged flat-field image FF (Figure 5(b)). BG_1 is acquired with an empty probe volume, i.e. nothing on top of the piston-top window.
3. Subtract an ensemble-averaged background image BG_2 (Figure 5(c)) from the corresponding averaged liquid-film image CD (Figure 5(d)). BG_2 is acquired with the calibration device filled neat iso-octane, i.e., surrogate fuel without tracer.
4. Divide the result of (3) by that of (2) pixel-wise, field-wide. Figure 5(e) shows the result for the example ensembles.

The spatial standard deviation of the corrected LIF image in Figure 5(e) is 9 %. Since the calibration device itself may not provide a perfectly uniform film thickness, this value is an upper limit of the expected precision uncertainty. From the manufacturer-specified tolerances of the precision shims and the fused silica windows, the accuracy of setting a target film thickness in the calibration device is estimated to be 16 %.

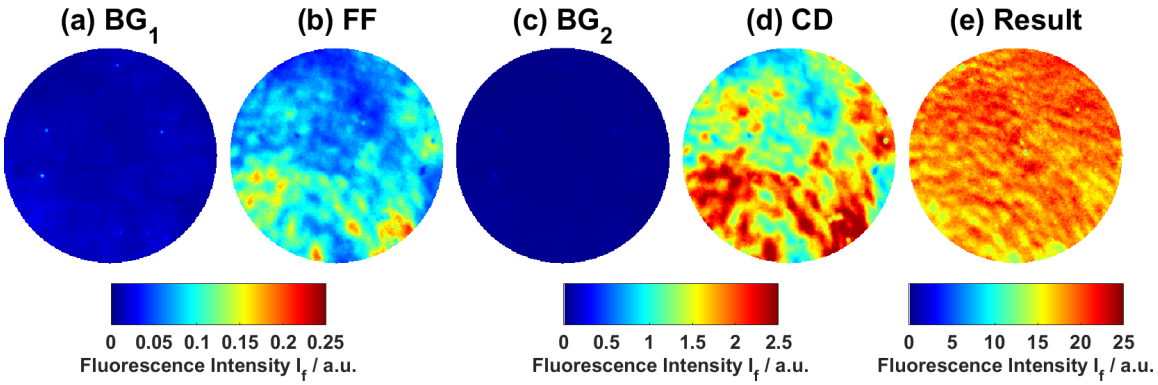

Figure 5. Post-Processing for a film of iso-octane/toluene-mixture: (a) Background for the flat-field: empty measurement volume, (b) flat-field, (c) Background 2: calibration device filled with isooctane (d) Film image: calibration device filled with toluene and isooctane. (e) Result of the post-processing. Fluorescence intensity is given in arbitrary but consistent units.

The flat-field correction assumes that the transverse profile of the laser light does not change over the time it takes to acquire the four image ensembles, in particular not between images FF and CD. Any such change reduces the precision, but (to first order) does not introduce additional inaccuracy with respect to the image-wide mean value, since the total pulse energy is accounted for in step (1).

Tracer characterization

For this study, iso-octane (99 °C) was chosen as the surrogate fuel. It has been used in many previous investigations [13, 27, 28, 29]. Concerning the fluorescent tracer, a number of criteria have to be considered. To ensure co-evaporation between tracer and surrogate fuel, it is advantageous for the tracer to have similar physical properties as the surrogate fuel. The tracer's spectral properties should be known and compatible with the available laser and camera technology. The fluorescence red shift needs to be sufficiently large for spectral separation from the incident laser light. For a reasonable signal to noise ratio, the fluorescence quantum yield and the extinction coefficient at the excitation wavelength should be sufficiently high. The tracer should not decompose under the laser irradiation. Finally, some tracers, e.g. benzene, are too difficult to handle in compliance with typical engine-laboratory safety rules.
Here, we considered toluene and 3-pentanone as candidates for a liquid-film tracer. As discussed in the introduction, both have been used extensively in previous research, mainly, because their boiling points are similar to that of iso-octane (111 and 102 °C, respectively. However, their molecular structure is very different from each other and also from iso-octane. As opposed to 3-pentanone, toluene commonly is found in commercial and certification gasoline.

Signal non-linearities

The film thickness of various mixtures of iso-octane and tracer was varied in calibration device 1 at room temperature and pressure. Within the circular field of view (FOV) of a post-processed ensemble-averaged image (see Figure 5(e)), the LIF signal in each of 64 sub-areas of 20 x 20 pixels distributed across the FOV was averaged. For toluene, Figure 6 shows the median of those 64 values and their standard deviation as an error bar. Fuel film thicknesses ranged from 40 µm to 200 µm for 0.25 – 1 % toluene by volume and up to 300 µm for concentrations of 2.5 % and 5 %. A first inspection of Figure 6 shows that over the range investigated here, the signal is in good approximation linear with film thickness for 0.25, 0.5, and 1 % toluene, while this is clearly not the case for 2.5 % and 5 %. In fact, at 5% concentration, the measured signal saturates at 150 µm film thickness, i.e., increasing thickness does not lead to further significant increase of the signal.

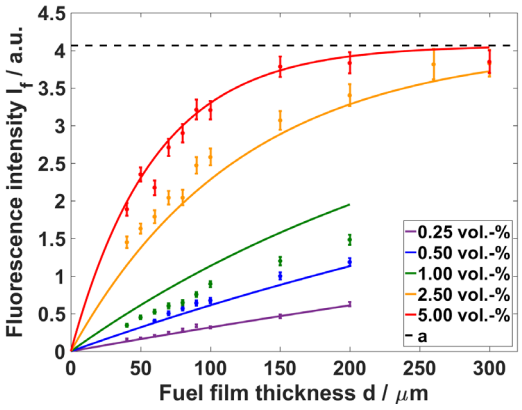

Figure 6. Variation of liquid film thickness for different concentrations of toluene in iso-octane. Solid lines represent the global fit to the Lambert-Beer (equation (4)).

In a next step we investigated how well the data are described by the (exponential) Lambert-Beer law expressed in equation (1). The flat-field corrected fluorescence is described by equation (4).

$$I_{f^*} = \frac{I_{f,CD}}{I_{f,FF}} = \frac{(\eta \cdot \phi \cdot I_0 \cdot (1-exp(-\epsilon^* \cdot c \cdot d)))_{CD}}{(\eta \cdot \phi \cdot I_0 \cdot (1-exp(-\epsilon^* \cdot c \cdot d)))_{FF}} = a \cdot (1 - exp(-\epsilon^* \cdot c \cdot d))_{CD} \qquad (4)$$

Here, the "transfer factor" a summarizes those parts of the relation between calibration-device-LIF and flat-field-LIF that do not change with the molar concentration c, the extinction coefficient ϵ^*, and the thickness d of the fuel film. Equation (4) was fit to the entire data set of all concentrations and film thicknesses represented in Figure 6 with a and ϵ^* as fit parameters. This global fit represents the data well, except for the case of 1% toluene. A possible error source could be the toluene concentration in the mixture, since all points in one concentration series were based on the same mixture. Note that the error bars only represent the precision of the measurement, not its accuracy. Overall, the coefficient of determination is 97.64 %, and the extinction coefficient ϵ^* of toluene is found to be 538.63 dm³/(cm mol). This value corresponds to a decadic extinction coefficient of 233.9 dm³/(cm mol) for pure toluene. Lin and Sick [13] found a comparable value of 280 dm³/(cm mol) for toluene in iso-octane at room temperature at 266 nm, while from Berlman's absorption spectra for toluene in cyclohexane, at 266 nm, a value of 180 dm³/(cm mol) can be read [36].The fit yields a transfer factor a = 4.0646 (at room temperature and pressure, which were the ambient conditions for this investigation). For an intended range of fuel-film thicknesses, Figure 6 or equivalently equation (4) can be employed to determine which maximum tracer concentration to use if the measurement is to remain within a given linearity error.

Figure 7 shows the corresponding results for 3-pentanone. In this case, the minimum concentration was chosen to be 5 % by volume, because the extinction coefficients of ketones are generally much lower than those of aromatic species. Fitting equation (5) to this data set yielded an extinction coefficient ϵ^* = 50.11 dm³/(cm mol) and a = 0.61, with a coefficient of determination of 96.57 %. This value of ϵ^* corresponds to a decadic extinction coefficient of 21.76 dm³/(cm mol). Ossler et al. [37] give a value of 19 dm³/(cm mol) for pure 3-pentanone and slightly elevated temperature (323 K).

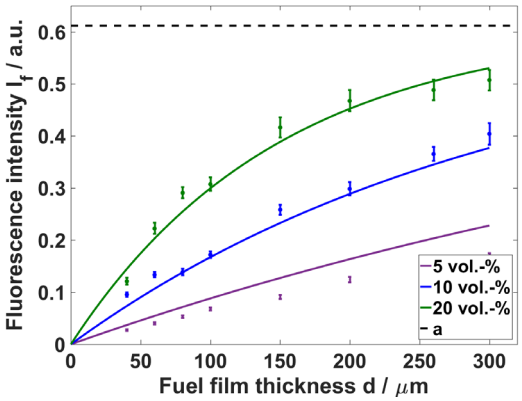

Figure 7. Variation of liquid film thickness for different concentrations of 3-pentanone in iso-octane. Solid lines represent the global fit to the Lambert-Beer (equation (4)). The values for fluorescence signal (on the y-axis) are consistent with those in Figure 6.

As expected, there is a large difference in fluorescence signal between 3-pentanone and toluene. For a concentration of 5 % by volume and the thinnest films investigated here, where the signal scaling is still somewhat close to linear for both tracers, the signal from 3-pentanone is almost two orders of magnitude lower. Consequently, as in gas-phase LIF measurements [31], much higher 3-pentanone concentrations would be needed to ensure a reasonable single-shot signal-to-noise ratio. For example, Schulz et al. [29] used 3-pentanone of 12 % by volume in iso-octane for their investigations.
Adding high concentrations of a "non-natural" fuel component may significantly change the ignition and combustion properties of the surrogate/tracer-mixture compared to a standard gasoline fuel. Our reference fuel, a certification gasoline fuel for Euro 4, contains 8 % toluene. However, at a toluene concentration of 8 % the LIF signal would severely deviate from linear scaling with fuel-film thickness already at 50 µm thickness, which could well occur in engine operation. Thus, for further investigation a toluene concentration of 0.5 % and a 3-pentanone concentration of 5 % were chosen.

Influence of pressure

For this investigation, Version 2 of the calibration device is pressurized by nitrogen to 1 bar to 14 bar. For toluene and 3-pentanone, the detected fluorescence signal, for each tracer normalized by its value at 1 bar, is plotted in Figure 8.

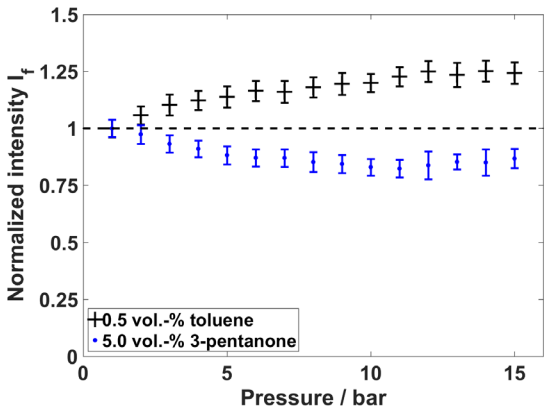

Figure 8. Pressure dependencies of toluene and 3-pentanone fluorescence at 20°C. Intensities are normalized by the values at ambient pressure.

For both tracers, a moderate influence of pressure on fluorescence intensity is found, but while at 15 bar for 3-pentanone the signal is 20 % lower than its room-pressure value, for toluene it is higher by that amount. Because of the incompressibility of the liquid phase, this effect cannot be caused by a change of density. We suspect the effect is due to dissolved oxygen. When the calibration tool is pressurized by nitrogen, the oxygen content of the fuel is reduced, presumably reducing the quenching rate. Preliminary experiments with a degassed mixture show reduced pressure dependence. However, even when injecting degassed fuel in the engine, it is not clear to what extent the gases in the cylinder are dissolved in the fuel as the spray droplets travel through the gas.

Influence of film temperature

Also in version 2 of the calibration device LIF from the tracer/iso-octane mixtures was investigated at temperatures up to 150 °C. Since this is much higher than the standard-pressure boiling points of iso-octane (99 °C), toluene (111 °C), and 3-pentanone (102 °C), the measurements were performed at 14 bar. The results in Figure 9 show significant influence of temperature on fluorescence intensity. LIF emission decreases with increasing temperature, much more so for toluene than for 3-pentanone. Increasing the temperature from 20 °C to 130 °C lead to a decrease of toluene fluorescence by a factor of five. This trend is consistent with gas-phase measurements with this tracer [38]. For 3-pentanone, the signal decreased to 65 % of its room-temperature value. Note that both data series are normalized by their room-temperature values. The absolute intensity of toluene fluorescence was much higher than that from 3-pentanone, also for the highest temperatures.

The results show that information on film temperature is needed for accurate film-thicknesses quantification. Compared to pressure, the temperature dependency is a greater challenge, since no standard instrument is available to measure the film temperature, in particular not with spatial resolution. In addition, temperature could be a function of the depth inside of the liquid fuel-film.

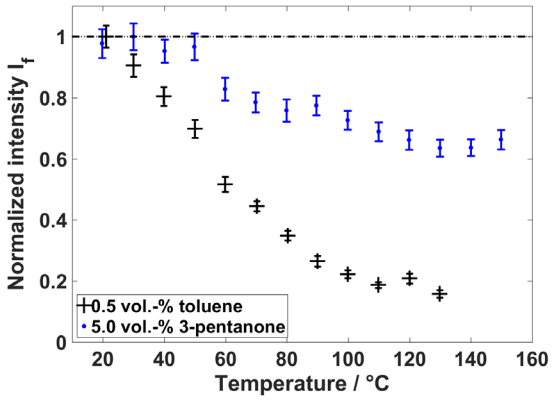

Figure 9. Temperature dependencies of toluene and 3-pentanone fluorescence at 14 bar. Intensities are normalized by values at room temperature.

Engine experiments

Experiment

The investigations were performed in an optically accessible single-cylinder engine with the characteristics presented in Table 1. The engine has a typical automotive four-valve, pent-roof head with a flat piston top. Optical access is through the cylinder line and a window in the extended Bowditch-type piston. Fuel is injected directly (GDI) into the cylinder from a centrally mounted 6-hole injector. Port-fuel injection (PFI) with a high-pressure injector can also be used to create a nearly homogeneous mixture. Mass-flow controllers supply the intake with the desired mixture of air and nitrogen.

The operating conditions are listed in Table 1. Operation was motored with an intake pressure of 1000 mbar, which was slightly above ambient and exhaust conditions to avoid reverse blow-by (air flow from the environment into the combustion cylinder). The engine coolant and oil temperature was 80 °C. A relatively low engine speed of 600 rpm was chosen to be able to image every working cycle, given a maximum recording frequency of 5 Hz. In order to completely flush any remaining tracer from the cylinder before imaging, the engine was operated with injection in every fifth cycle. Phase-locked at a given crank angle (CA), a series of 200 images (in 200 cycles) was recorded, 40 images with injection and 160 without injection. The background image for subsequent post-processing was the average of the 40 images in each cycle preceding the one with injection.

Table 1. Characteristics of the engine and motored operating point. Valve timings are taken at 0.15 mm lift.

Displacement	449 cc
Stroke	85 mm
Bore	82 mm
Compression ratio	10.5:1
Number of valves	4
Injector position	Central (GDI), PFI
Injector	Bosch HDEV 5 (six holes)
Injection pressure	50, 100, 200 bar
Fuel	Iso-octane + 0.5 % toluene
Start of injection	360° CA BTDC
Exhaust valve open	126° CA ATDC
Exhaust valve close	360° CA ATDC
Intake valve open	358° CA BTDC
Intake valve close	138° CA BTDC
Engine speed	600 1/min
Intake pressure	1000 mbar
Intake temperature	30 °C
Oil temperature	80 °C
Cooling water temperature	80 °C

The optical arrangement on the engine test bench was essentially that presented in Figure 1. In addition, the measured fluorescence and absorption spectra of toluene are given. While the fluorescence spectrum was measured as described in the section “flat-field correction”, the absorption spectrum was measured in a cuvette at reduced concentration in a PerkinElmer Lambda25-spectrometer. An overview of the spectral features of LIF excitation and detection is given in Figure 10. Whereas in the bench-top experiments a long-pass filter rejected laser-light reflections, in the engine experiments a band-pass filter (Semrock FF01-292/27-25) was used instead. This filter was found to effectively suppress background fluorescence from the engine head. It also restricts the spectral

range of detection to the part of the fluorescence spectrum that does not overlap with the excitation spectrum.
The high LIF signal level from only 0.5 % toluene in the liquid phase allows setting the lens to a small aperture. At f/5.6, the depth of focus extended over the whole piston stroke of 85 mm. Thus, the camera does not need be refocused or moved for different image acquisition at different crank angles. The image intensifier was operated at a gain of "40", as set in the camera operating software DaVis (LaVision).

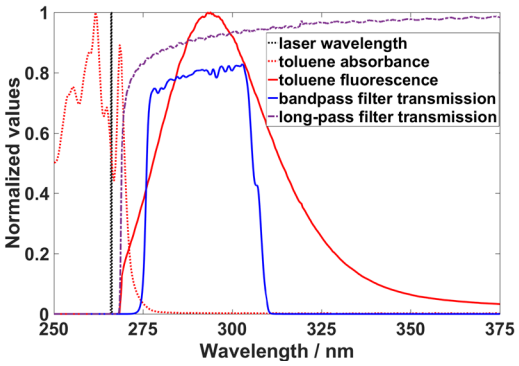

Figure 10 Transmission spectrum of the detection filter in relation to the fluorescence and absorption spectra of toluene (filter transmission data from data sheets [39, 40]).

The flat-field correction was performed as described in section "Post-processing". For an absolute calibration, Version 1 of the calibration device was placed on the piston top and images at film thicknesses between 10 and 160 µm were acquired and flat-field corrected. Assuming a linear correlation between fluorescence signal and film thickness for this range, a fit to measurement results yielded

$$d(x,y) = I_{f*}(x,y) \cdot 8.2044 - 1.9553\ \mu\text{m}. \quad (5)$$

The offset of about 2 µm is due to inaccuracies in setting each film thickness and imperfect background correction. We did not force the fit through (0,0) because this would have altered its slope. The offset is then an estimate of the detection limit in terms of measurement accuracy.

Results

Influence of bulk gas composition

To study fuel films on the piston surface, the engine was operated in GDI mode, injecting 24 mg per cycle of iso-octane + 0.5 % toluene at 200 bar with a start of injection of 360° CA BTDC (= gas exchange TDC). Figure 11 shows the fuel-film thickness imaged at 300° CA BTDC for (a) air (21 % oxygen) and (b) nitrogen (0 % oxygen). In both images, the "fingerprint" of the spray is visible as six lobes of wetted area on the piston top. The maximum film thicknesses are about 60 µm and they are found near the borders of the fuel film. Between the image with nitrogen as the bulk gas (b) and that with air (a), the former shows an offset of about 10 µm across the entire field of view. This is

presumably caused by gas-phase fluorescence. Quenching of gas-phase fluorescence was investigated next.

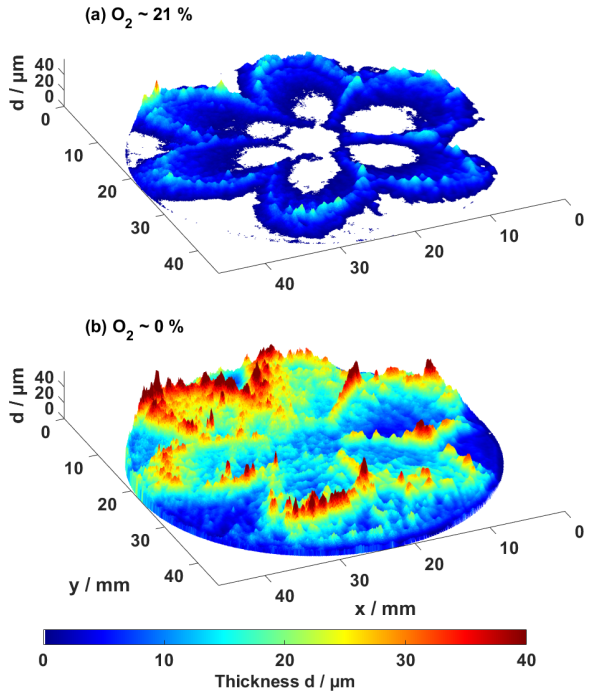

Figure 11. Measured fuel-film thickness on the piston surface at 300° CA BTDC for air (top) and nitrogen (bottom) as a bulk gas.

To study the effect of quenching by oxygen on the gas-phase fluorescence, the engine was operated in PFI mode. The fuel was injected into the intake manifold by a multi-hole injector at 400° CA BTDC (i.e., before intake-valve opening) with an injection pressure of 100 bar.

While there was no significant LIF signal for air as the bulk gas, in nitrogen the gas-phase fuel was detectable. Based on equation (6), the intensity of this gas-phase fluorescence can be converted to an equivalent liquid film thickness, shown in Figure 12. The average over the field of view is 15 µm. Thus, in nitrogen, the film thickness may be overestimated by up to this value for the given injection quantity.

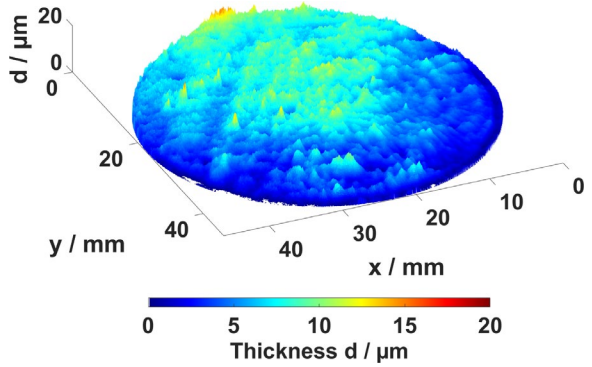

Figure 12. Equivalent liquid film thickness corresponding to LIF from the gas phase with PFI in nitrogen. Image timing: 300° CA BTDC.

Application example: rail pressure variation

As a simple application example, fuel films over a variation of rail pressures at the same start of injection (360° CA BTDC) were investigated. For pressures of 50 bar, 100 bar, and 200 bar, the injection duration was adjusted to equalize the injected fuel mass. Air was used as the bulk gas (but operation was still motored).

Figure 13 shows the resulting fuel films at 300° CA BTDC. The six-lobed shape of the fuel film and the total wetted area is similar for all three injection pressures. The fuel film thickness increases from the center to the edge of each lobe for all injection pressures. The momentum of the injection seems to push the liquid film towards the edges, where maximum fuel-film thicknesses of 60 µm occur for 50 and 100 bar and 40 µm for 200 bar. While typical thicknesses appear similar for 50 bar und 100 bar, injecting at 200 bar reduces the film. As Figure 6 showed, with a toluene concentration of 0.5%, for 60 µm film thickness there is no significant deviation from a linear relation with LIF intensity. In fact, toluene could have been added at significantly higher concentrations.

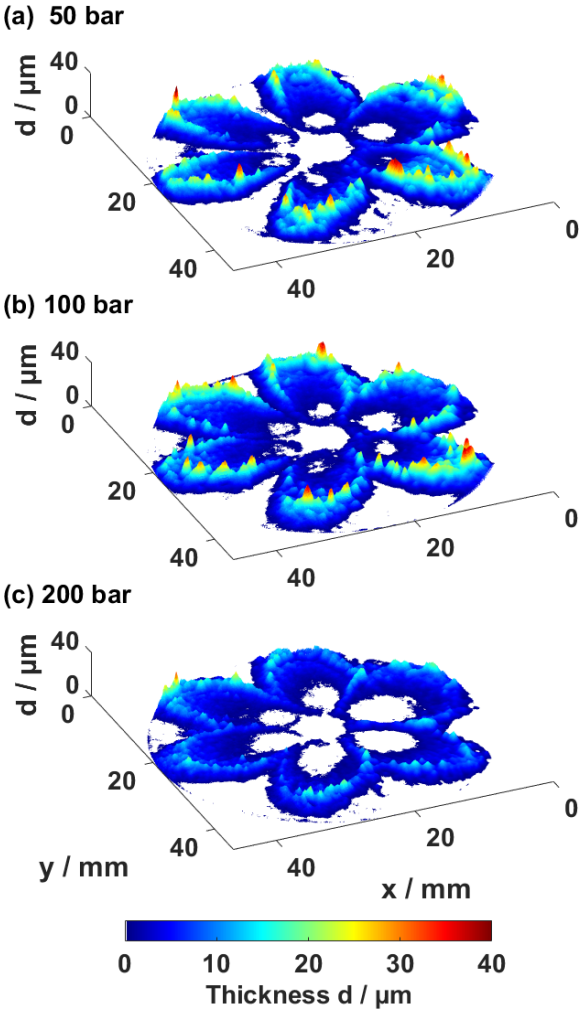

Figure 13. Fuel-film thickness on the piston surface for different injection pressures (image timing: 300° CA BTDC).

Results from a crank-angle series for 50 bar rail pressure are shown in Figure 14. At 350° CA BTDC, injection has ended, but a large portion of the spray has still neither evaporated nor impinged on the piston. This was confirmed by additional imaging from the side (not shown here), but can also be deduced from the rapid change of the structure of the 6 lobes from 350 to 340° CA BTDC that is consistent with the spray still partly travelling through the combustion chamber. From 340° CA BTDC on, the images show essentially only the film on top of the piston. No fuel is found in the center of image, whereas at 350° CA BTDC strong signal is detected here. As expected, the thickness monotonically decreases with time, while the film remains in its original position. Those regions that initially had the least liquid are dry first.

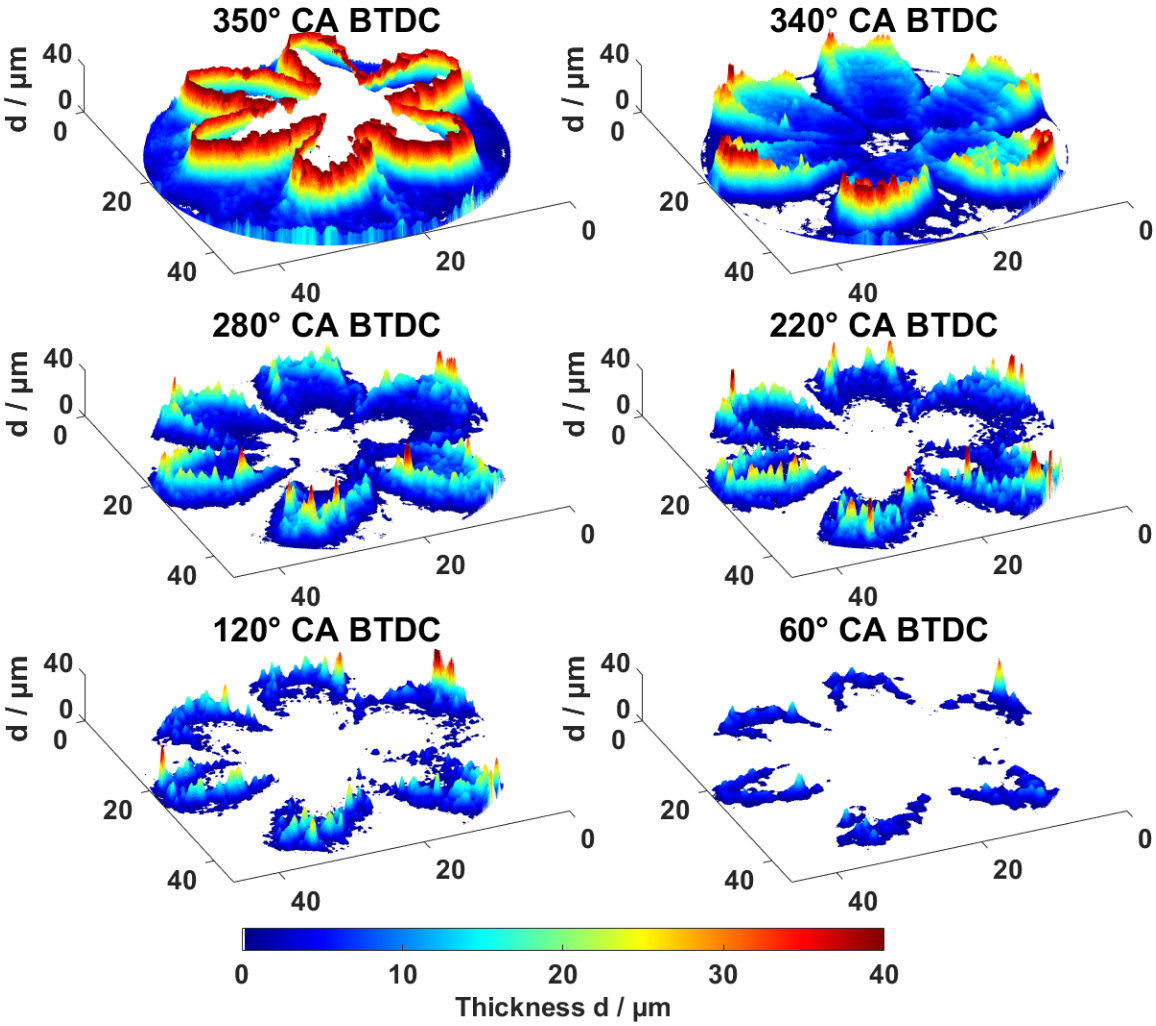

Figure 14. Crank-angle series of LIF images converted to fuel-film thickness on the piston top as a function for injection with 50 bar. Note that at 350° CA BTDC the LIF signal comes partly from the spray, not only the film, as discussed in the text.

For further analysis the total mass of the fuel film at each crank angle was calculated by integration over the FOV and assuming a constant liquid density of 690 kg/m³ (iso-octan at room temperature).

In Figure 15 this fuel-film mass is shown normalized by the total injected mass (which was constant for all injection pressures). The data series start at 340° CA BTDC, when film formation is complete for all pressures. For a rail pressure of 50 bar, initially 38 % of the total fuel mass is detected on the piston top. As indicated by Figure 13, an increase of the injection pressure from 50 bar to 100 bar does not significantly reduce the fuel mass deposited on the surface, but upon further doubling to 200 bar only 25 % of the injected mass are found on the piston top, a reduction by 32 %. This is consistent with the results of Schulz et al. [29] in a constant-pressure vessel, where for comparable ambient conditions increasing pressure from 50 to 150 bar also did not result in less mass on the surface below 25 mm the injector, whereas 300 bar did. For both 50 and 200 bar the film mass monotonically decreases with time, with the last significant amount of fuel detected at 180° CA BTDC for 200 bar and 60 for 50 bar. The last increment of this decrease appears to be somewhat inconsistent with the previous trend for both traces. This could be attributable to the aforementioned limited accuracy for very thin films. At all crank angles the rate of decrease, i.e., of film evaporation, is greater for 200 bar rail pressure, in particular for earlier crank angles. This is consistent with the higher initially deposited fuel mass (for 50 bar) cooling the piston top more.

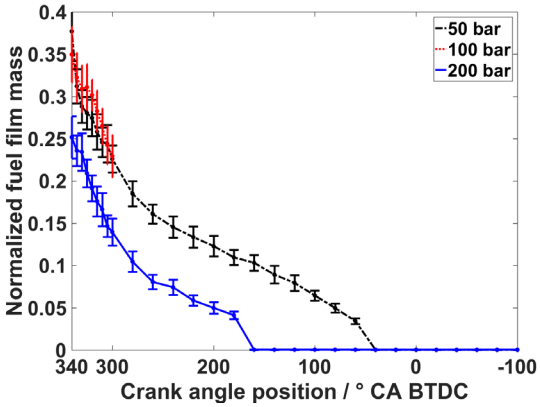

Figure 15. Fuel-film mass as a fraction of the injected mass as a function of crank angle during compression and early expansion.

In particular for early crank angles after injection, the measurements could have inaccuracies stemming from very fuel rich zones (in the extreme, residual droplets) where the spray just has evaporated. If their oxygen concentration is low enough, fluorescence is not quenched efficiently, and the gas phase contributes to the detected signal, as it does in nitrogen atmosphere. Additionally, note that these results are not corrected for temperature, which was shown above to have an effect on the LIF signal.

Conclusions and future work

Based on laser-induced fluorescence imaging of a tracer added to a non-fluorescing surrogate fuel, a procedure for measuring the liquid fuel-film thickness on transparent surfaces of optically accessible research engines was developed. While it is quite easy to obtain qualitative images, quantification requires further investigations.

The first part of this work deals with bench-top experiments on the photo-physics of two potential tracers, toluene and 3-pentanone. For this purpose, rugged thin-film cuvettes were designed, which allow investigating the liquid-film fluorescence over most of the range that is relevant in DI SI engines (up to 180 °C and 16 bar).
The relation between fluorescence signal intensity, tracer concentration, and fuel-film thickness was investigated for toluene and 3-pentanone dissolved in iso-octane. As expected from literature results on gas-phase LIF, the signal from toluene is much stronger than from 3-pentanone. For films thinner than 100 µm, a reasonable 3-pentanone concentration might be 5 – 10 %, but less than 1 % toluene.
Next, the fluorescence signal behaviour of toluene and 3-pentanone at elevated temperature and pressure was investigated. Significant differences were found with respect to temperature. At 130 °C the LIF signal from toluene is about 20 % of that at 20 °C, but still 70 % from 3-pentanone. These trends are qualitatively consistent with what is known for the gas phase. Thus, the temperature of the fuel wall film needs to be known for fully quantitative results.
Apart from the influence of tracer photophysics, for image quantification the spatial non-uniformity of laser excitation and detection efficiency needs to be taken into account. This "flat-field correction" was performed using a fluorescing solid disk instead of a liquid film, which significantly simplifications the calibration process. A Schott-glass WG280 long-pass filter was found to be a suitable and inexpensive flat-field material.
The second part of the paper presents result from an initial application in a motored DI SI engine with a central injector, actuated at gas-exchange TDC when the piston is close to the injector and fuel impingement can be expected. Iso-octane with 0.5 % toluene were used as a surrogate fuel, injecting at 50, 100, and 200 bar rail pressure into air or nitrogen fed to the engine running at 600 rpm with 1 bar intake pressure.
With nitrogen as a bulk gas, fluorescence from evaporated fuel introduces an offset in the liquid-film measurement, while in air gas-phase fluorescence is efficiently quenched by oxygen. We conclude that an oxygen-containing bulk gas may increase the accuracy of the film-thickness measurement by suppressing fluorescence from already evaporated fuel. However, possible quenching of the liquid phase has not been considered yet.
Consistent with recent work in a constant-pressure vessel [29], the film was thickest at its outer edge for all conditions and increasing rail pressure did not necessarily decrease piston wetting. Instead, at 50 and 100 bar the initial film had nearly equal total mass, but further increase to 200 bar rail pressure decreased the fuel mass deposited on the piston. The evaporation history was then very similar for 50 and 200 bar. The thinner film finished evaporation earlier, as expected.
Two issues for further investigation and improvement of this LIF technique stand out: determining the temperature of the film to account for its influence on LIF imaging, and a more realistic surrogate fuel. Concerning the former, we are investigating if, as is the case in the gas phase, there is some dependency of the fluorescence spectrum on liquid temperature that could be exploited for temperature imaging. As for the latter, the surrogate fuel should approximate the boiling curve of reference gasoline as well as possible. Iso-octane only, because low-volatility components are not represented, may not be representative for gasoline in terms of initial wetting and subsequent evaporation. For a multi-component surrogate, suitable tracers would then need to be identified with the help of the thin-film cuvettes developed in this work.

Acknowledgements

The experiments were performed at Bosch Corporate Research Facility, Renningen, Germany. The authors gratefully acknowledge the contributions of Andreas Herzig, Bernd Hüttl, Ralf Köhler, and Martin Noack for their assistance in maintaining the lasers and research engine used in this study.

Declaration of conflicting interests

The authors declare that there is no conflict of interest.

Funding

This project has received funding from the European Union's Horizon2020 Programme for research technological development and demonstration under Grant Agreement no. 723954.

References

1. Steimle F, Kulzer A, Richter H, et al.. Systematic Analysis and Particle Emission Reduction of Homogeneous Direct Injection SI Engines. SAE Technical Paper 2013-01-0248, 2013.

2. Drake M, Fansler T, Solomon A, et al.. Piston Fuel Films as a Source of Smoke and Hydrocarbon Emissions from a Wall-Controlled Spark-Ignited Direct-Injection Engine. SAE Technical Paper 2003-01-0547, 2003.

3. Stojkovic BD, Fansler TD, Drake MC et al.. High-speed imaging of OH* and soot temperature and concentration in a stratified-charge direct-injection gasoline engine. Proceedings of the Combustion Institute 2005; 30: 2657 – 2665.

4. Ma X, He X, xin Wang J., et al.. Co-evaporative multi-component fuel design for in-cylinder PLIF measurement and application in gasoline direct injection research. Applied Energy 2011; 88: 2617 – 2627.

5. De Sercey G, Heikal M, Gold M, Begg, et al.. On the use of laser-induced fluorescence for the measurement of in-cylinder air-fuel ratios. Proceedings of the

Institution of Mechanical Engineers, Part C: Journal of Mechanical Engineering Science 2002; 216: 1017-1030.

6. Zhao H and Ladommatos N. Optical diagnostics for in-cylinder mixture formation measurements in IC engines. Progress in Energy and Combustion Science 1998; 24: 297 – 336.

7. Wensing, M, Günther M, Zboralski A, et al.. Endoskopische laserinduzierte Fluoreszenz in der Brennverfahrensentwicklung. MTZ - Motortechnische Zeitschrift 2014; 75: 44-51.

8. Schulz C and Sick V. Tracer-LIF diagnostics: quantitative measurement of fuel concentration, temperature and fuel/air ratio in practical combustion systems. Progress in Energy and Combustion Science 2005; 31: 75 – 121.

9. Senda J, Ohnishi M, Takahashi T, et al.. Measurement and Modeling on Wall Wetted Fuel Film Profile and Mixture Preparation in Intake Port of SI Engine. SAE Technical Paper 1999-01-0798, 1999.

10. Takahashi Y, Nakase Y and Ichinose H. Analysis of the Fuel Liquid Film Thickness of a Port Fuel Injection Engine. SAE Technical Paper 2006-01-1051, 2006.

11. Schropp PP. Optische Methoden zur Bewertung des Kolbenwandfilms in Benzinmotoren mit Direkteinspritzung. Diploma Thesis, Karlsruher Institut für Technologie, Germany, 2013.

12. Grzeszik R. Optische Messtechniken zur Bewertung innermotorischer Wandfilme. In: 9. Tagung Diesel- und Benzindirekteinspritzung, Berlin, Germany, 3 December – 4 December 2014, pp. 385-400. HDT.

13. Lin M and Sick V. Is Toluene a Suitable LIF Tracer for Fuel Film Measurements?. SAE Technical Paper 2004-01-1355, 2004.

14. Tibiriçá CB, do Nascimento FJ and Ribatski G. Film thickness measurement techniques applied to micro-scale two-phase flow systems. Experimental Thermal and Fluid Science 2010; 34: 463 – 473.

15. Al-Sibai F. Experimentelle Untersuchung der Strömungscharakteristik und des Wärmeübergangs bei welligen Rieselfilmen. PhD Thesis, University RWTH Aachen, Germany, 2004.

16. Sherrington I, Smith EH. Experimental Methods for Measuring the Oil-film Thickness between the Piston-rings and Cylinder-wall of Internal Combustion Engines. Tribology International 1985; 18.

17. Sun RK, Kolbe WF, Leskovar B and Turko B. Measurement of Thickness of thin Water Film in Two-phase Flow by Capacitance Method. IEEE Transactions on Nuclear Science 1982; NS-29:1.

18. Schulz F, Schmidt J, Kufferath A, Samenfink W. Gasoline Wall Films and Spray/Wall Interaction Analyzed by Infrared Thermography. SAE Int. J. Engines 2014; 7(3):1165-1177, 2014.

19. Le Coz JF, Baritaud T. Application of laser induced fluorescence for measuring the thickness of evaporating gasoline liquid films. In: Developments in laser techniques and applications to fluid mechanics 1996, pp. 115–131.

20. Fansler TD and Drake MC. "Designer diagnostics" for developing direct-injection gasoline Engines. Journal of Physics: Conference Series 2006; 45, 1.

21. Maligne D and Bruneaux G. Time-Resolved Fuel Film Thickness Measurement for Direct Injection SI Engines Using Refractive Index Matching. SAE Technical Paper 2011-01-1215, 2011.

22. Hewitt GF. Disturbance waves in annular two-phase flow. In: Proc Inst Mech Eng Conf Proc 1996, paper no. 184(33), pp. 142–150.

23. Senda J, Ohnishi M, Takahashi T, Fujimoto H.. Measurement and Modeling on Wall Wetted Fuel Film Profile and Mixture Preparation in Intake Port of SI Engine. SAE Technical Paper 1999-01-0798, 1999.

24. Takahashi Y, Nakase Y and Ichinose H.. Analysis of the Fuel Liquid Film Thickness of a Port Fuel Injection Engine. SAE Technical Paper 2006-01-1051, 2006.

25. Stevens E and Steeper R. Piston Wetting in an Optical DISI Engine: Fuel Films, Pool Fires, and Soot Generation. SAE Technical Paper 2001-01-1203, 2001.

26. Kull E, Wiltafsky G, Stolz W, Min KD and Holder E. Two-dimensional visualization of liquid layers on transparent walls. Opt. Letters 1997; 22: 645-647.

27. Kay PJ, Bowen PJ, Gold M and Sapsford S. Development of a 2D quantitative LIF Technique towards Measurement of Transient Liquid Fuel Films. In: Proceedings of 10th International Congress on Liquid Atomization and Spray Systems, Cardiff, Wales, 2006, available from: http://eprints.uwe.ac.uk/26359.

28. Schulz F, Schmidt J and Beyrau F. Development of a sensitive experimental set-up for LIF fuel wall film measurements in a pressure vessel. Experiments in Fluids 2015; 56.

29. Schulz F, Samenfink W, Schmidt J and Beyrau F. Systematic LIF fuel wall film investigation. Fuel 2016; 172: 284 - 292.

30. Fujikawa T, Hattori Y, Koike M, et al.. Quantitative 2D fuel distribution measurements in a direct-injection gasoline engine using a laser-induced fluorescence technique. JSME Int J 1999; 42(4):760–767.

31. Koban W. Photo physical characterization of toluene and 3-pentanone for quantitative imaging of fuel/air ratio and temperature in combustion systems. PhD Thesis, University of Heidelberg, Germany, 2005.

32. Yang J and Melton LA. Fluorescence-Based Method Designed for Quantitative Measurement of Fuel Film Thickness during Cold-Start of Engines, Applied Spectroscopy 2000; 54.

33. Alonso M, Kay PJ, Bowen PJ, Gilchrist R, Sapsford S. A laser induced fluorescence technique for quantifying transient liquid fuel films utilizing total internal reflection. Exp Fluids 2010; 48: 133 – 142.

34. Cho H and Min K. Measurement of liquid fuel film distribution on the cylinder liner of a spark ignition engine using the laser-induced fluorescence technique. Measurement Science and Technology 2003; 14, 975.

35. Eckbreth AC. Laser diagnostics for combustion temperature and species. 2th ed. Gordon and Breach Publ., 1996.

36. Berlman IB. Handbook of Fluorescence Spectra of aromatic molecules. 2th ed. Academic Press, 1971, pp. 117.

37. Ossler F and Adén M. Measurement of picosecond laser induced fluorescence from gas phase 3-pentanone and acetone: Implications to combustion diagnostics. Appl. Phys. B 1997, 64: 493-502.

38. Wermuth N and Sick V. Absorption and fluorescence Data of Acetone, 3-Pentanone, Biacetyl, and Toluene at Engine-Specific Combinations of Temperature and Pressure. SAE Technical Paper 2005-01-2090, 2005.

39. Semrock, Transmission spectra of 292/27 nm single-band bandpass filter, https://www.semrock.com/filterdetails.aspx?id=ff01-292/27-25, (2017, accessed May 2017).

40. Semrock, Transmission spectra of ultrasteep long-pass edge filter, https://www.semrock.com/filterdetails.aspx?id=lp02-266ru-25, (2017, accessed May 2017).